Polymer Chemistry

ROYAL SOCIETY OF CHEMISTRY

PAPER

View Article Online
View Journal

Check for updates

Cite this: DOI: 10.1039/d4py01253d

Synthesis of poly(3,4-propylenedioxythiophene) (PProDOT) analogues *via* mechanochemical oxidative polymerization†

Tanzida Zubair, Raul S. Ramos, Ashley Morales and Robert M. Pankow *

Conjugated polymers (CPs) are foundational materials in established and emerging organic electronic technologies, including organic photovoltaics, lithium-ion batteries, electrochromic displays and smart-windows, and thin-film transistors. Although CPs can be prepared *via* sustainable syntheses relative to their inorganic counterparts, current polymerization methods often invoke the use of toxic, hazardous solvents, such as toluene, chlorobenzene, or dimethylformamide, and high-temperatures (T > 100 °C) to afford polymer products in desirable yields and molecular weights (M_n). Here, we report the solvent-free synthesis of poly(3,4-propylenedioxythiophene) (PProDOT) analogues using mechanochemical oxidative polymerization without the application of external heating. PProDOT-OC6, which is functionalized with *n*-hexyloxy sidechains, is synthesized in 46% yield with a M_n of 16.9 kg mol^{-1} in 1 h using only a milling jar and ball, $FeCl_3$ oxidant, and NaCl as an additive. The structural fidelity of mechanochemically synthesized PProDOT-OC6 is confirmed *via* ^{1}H-NMR relative to PProDOT-OC6 synthesized using solvent based oxidative polymerization, in addition to the optical absorption and electrochemical properties. The optimal mechanochemical polymerization conditions are then applied to PProDOT analogues with extended, *n*-decyloxy (PProDOT-OC10) or oligo(ethylene glycol) sidechains (PProDOT-OEG$_3$) to demonstrate the tolerance of these solvent-free polymerization conditions towards structurally diverse sidechains. These findings offer a new platform and approach for further developing sustainable CP polymerization methods.

Received 5th November 2024,
Accepted 23rd January 2025

DOI: 10.1039/d4py01253d

rsc.li/polymers

Published on 28 January 2025. Downloaded by NIMS SENGEN LIB on 2/12/2025 4:19:03 AM.

Introduction

Conjugated polymers are a unique class of optically and electroactive organic materials that provide efficient, tuneable electronic transport (hole or electron), ion transport, and optical absorption suitable for use in organic photovoltaics,[1–3] organic field effect and electrochemical transistors,[4–6] lithium-ion batteries,[7,8] chemical sensors[9] and electrochromic devices.[10–12] In contrast to their inorganic counterparts, the preparation of conjugated polymers can be considered low-cost, scalable, and more sustainable.[13,14] Typical polymerization methods for the preparation of conjugated polymers include oxidative chemical polymerization, electrochemical oxidative polymerization, Kumada catalyst transfer polymerization (KCTP), Suzuki–Miyaura polymerization, Stille polymerization, and direct arylation polymerization (DArP) (Fig. 1).[15–17]

Although the synthetic procedures for the preparation of conjugated polymers are relatively benign to many inorganic materials, the polymerization methodologies often invoke toxic solvents [*e.g.* toluene, chlorobenzene (CB), tetrahydrofuran (THF), dimethylformamide (DMF), and dimethylacetamide (DMAc)], high-temperatures (≥100 °C), and prolonged polymerization times (>12 h).[18–20]

Across the field of conjugated polymer synthesis, there is growing research interest in the development of more sustainable, environmentally benign polymerization protocols by

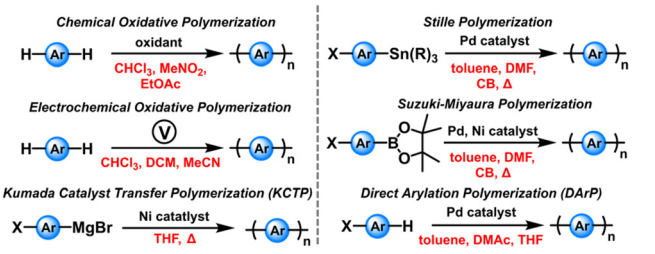

Fig. 1 Typical polymerization methodologies used for the synthesis of conjugated polymers.

Department of Chemistry and Biochemistry, University of Texas at El Paso, El Paso, Texas 79968, USA. E-mail: rmpankow@utep.edu

†Electronic supplementary information (ESI) available: Monomer synthesis and characterization, polymer synthesis and characterization. See DOI: https://doi.org/10.1039/d4py01253d

Published on 28 January 2025. Downloaded by NIMS SENGEN LIB on 2/12/2025 4:19:03 AM.

incorporating monomers from renewable feedstocks,[21–23] C–H functionalization,[24,25] recyclable conjugated polymers,[21,26,27] and earth abundant or recyclable catalysts for conjugated polymer synthesis.[14,28,29] However, in each these cases a toxic solvent is often employed in addition to high polymerization temperatures. More sustainably sourced solvents have been identified, such as 2-methyltetrahydrofuran (2Me-THF),[30,31] cyclopentyl methyl ether (CPME),[32] and *p*-cymene;[18] however, these solvents are still classified as hazardous and toxic compared to fully benign alternatives, *e.g.* water. Note, while water has been employed as a solvent for conjugated polymer synthesis, the broad scope utility remains relatively limited due to the specific functionalities required to impart water solubility for the monomers and conjugated polymer.[33–35] In order for conjugated polymer synthesis to better align with the central tenets of green chemistry, it is imperative that a new approach is undertaken.[36]

One approach towards more sustainable conjugated polymer synthesis includes mechanochemistry.[37–39] Mechanochemistry, *e.g.* manual grinding, ball milling, and extrusion, has been identified as a viable approach for small-molecule organic and inorganic materials; however, the application of mechanochemistry towards solution-processable conjugated polymer synthesis remains relatively unexplored.[40–42] Notable examples of mechanochemical polymerizations include, the synthesis of Schiff-base polymers,[43] linear and hyperbranched polypheneylenes,[44] hyperbranched polythiophenes,[45] polyacrylates,[46] and polyurethanes.[47] For conjugated polymers, identifying robust mechanochemical polymerization conditions suitable for a broad scope of monomer structures remains an outstanding challenge. Moreover, developing robust mechanochemical polymerization conditions for polythiophenes would be of significant benefit, since polythiophenes are incorporated into numerous device technologies throughout the field of organic electronics.[48,49]

In particular, poly(3,4-propylenedioxythiophene) (PProDOT) analogues are an emerging class of polythiophenes with applications in electrochromic devices,[50–52] lithium-ion batteries,[7,8] organic photovoltaics,[53] organic thermoelectrics,[54] and organic electrochemical transistors (Fig. 2).[55] PProDOT polymers are typically synthesized *via* Grignard metathesis (GRIM) polymerization,[56] solvent based oxidative polymerization,[51] or direct arylation polymerization (DArP) with PProDOT-C6, PProDOT-OEH, and PProDOT-OC6 as examples (Fig. 2A).[57] As previously noted, these polymerization methods all invoke the use of toxic solvents and high polymerization temperatures (up to 100 °C). Although the solvent-free oxidative polymerization has been explored for the synthesis of PProDOT-C6, separate manual grinding and thermal annealing (100 °C for 4 h) steps were required.[58] Additionally, extensive structural,

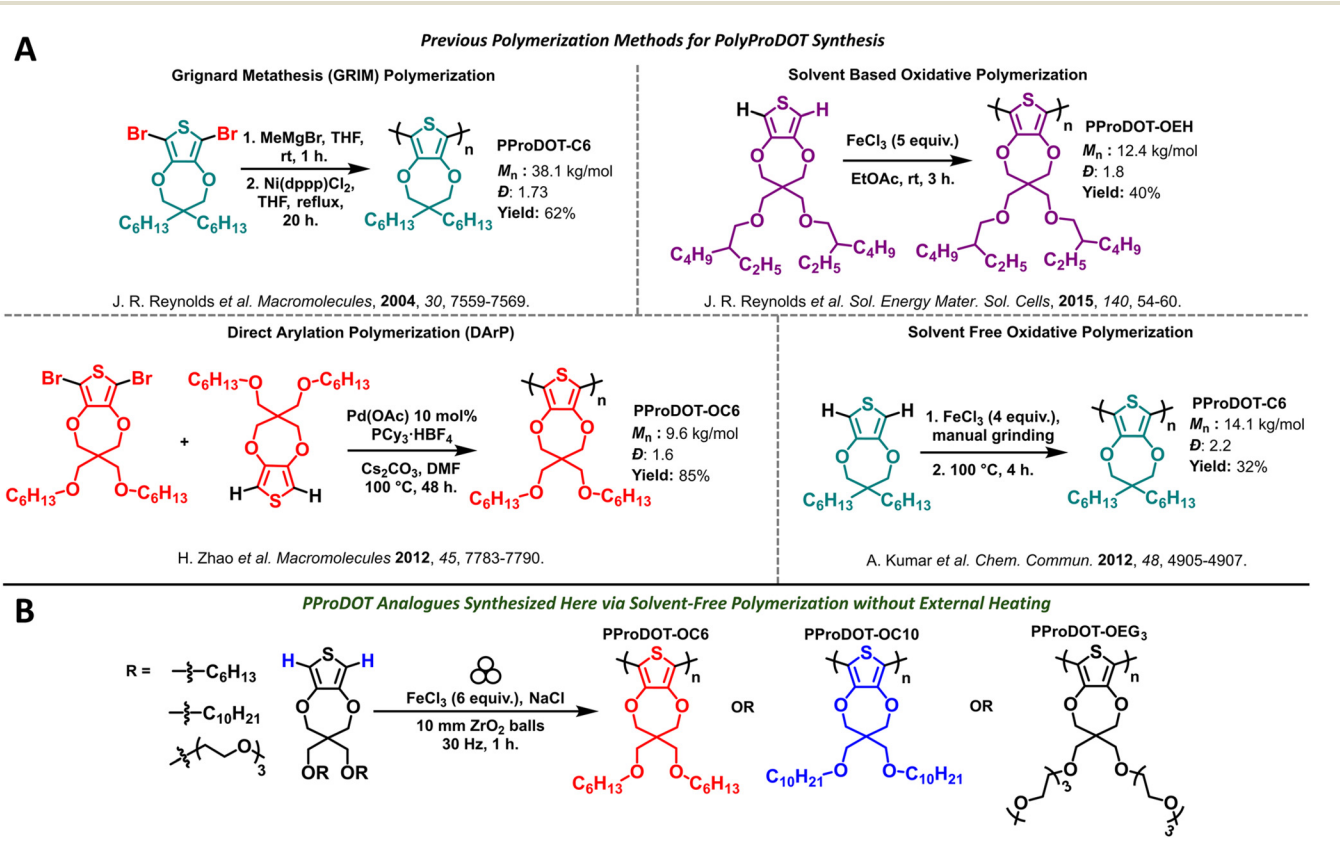

Fig. 2 (A) Previously reported polymerization methods towards the synthesis of PProDOT analogues including PProDOT-C6, PProDOT-OEH, and PProDOT-OC6. (B) Mechanochemical oxidative polymerization conditions reported here towards the synthesis of PProDOT-OC6, PProDOT-OC10, and PProDOT-OEG_3.

 This journal is © The Royal Society of Chemistry 2025

Published on 28 January 2025. Downloaded by NIMS SENGEN LIB on 2/12/2025 4:19:03 AM.

optical, and electrochemical characterization was not performed, and PProDOT analogues with varied sidechains were not investigated.

From the selected PProDOT analogues provided in Fig. 2A, there is a dependency of the polymer yield and M_n on the polymerization method employed. Specifically, for GRIM polymerization, which employs a highly reactive aryl Grignard reagent and nickel catalyst (analogous to KCTP), a yield of 62% with a M_n of 38.1 kg mol^{-1} is obtained for ProDOT-C6, and the yield and M_n notably drops for solvent based oxidative polymerization (40% and 12.4 kg mol^{-1}), DArP (85% and 9.6 kg mol^{-1}), and solvent free oxidative polymerization (32% and 14.1 kg mol^{-1}, respectively). Note, the solvent free oxidative polymerization affords a PProDOT product with broader $Đ$ ($Đ$ = 2.22) compared to the solvent based polymerization methods ($Đ$ = 1.6–1.8). Thus, there is ample space for the development and optimization of more sustainable polymerization conditions for this important class of conjugated polymers.

Here, the solvent-free synthesis of PProDOT analogues *via* mechanochemical oxidative polymerization without application of external heating is reported for the first time, to our knowledge. The polymerization proceeds under ambient conditions using a mixer mill and milling jar charged only with the monomer, $FeCl_3$, NaCl as an inert additive, and a single 10 mm mixing ball. After 1 h milling time, PPrODOT-OC6 is afforded in 46% with a M_n of 16.9 kg mol^{-1}. This is comparable to the yield and M_n achieved for PProDOT analogues using solvent based polymerization methodologies, *e.g.* DArP and oxidative polymerization (Fig. 2A and Table 1). To explore the effects of sidechain identity on the polymerization outcomes, PProDOT-OC10 and PProDOT-OEG_3, which have extended *n*-decyloxy and oligo(ethylene glycol) sidechains, respectively, were synthesized affording polymer products with acceptable M_n (14.0 and 7.6 kg mol^{-1}) and yields (44% and 32%). The polymers also possess narrow dispersity ($Đ$) ranging from 1.11–1.33. Additionally, the NMR, optical absorption, and cyclic voltammetry were performed to comprehensively assess the polymer structural, optical, and electrochemical properties. It was found that there is convergence between the PProDOT-OC6 synthesized using the optimal mechanochemical oxidative polymerization conditions and solvent based oxidative polymerization indicating that comparable structural fidelity can be achieved between the solvent-free and solvent based polymerization methods. Overall, the findings of this study and extensive analysis of the synthesized polymer products demonstrate the viability of mechanochemical polymerization methods for the sustainable synthesis of PProDOT analogues.

Results and discussion

In this section the optimization of the mechanochemical polymerization conditions towards the synthesis of PProDOT-OC6, PProDOT-OC10, and PProDOT-OEG_3 is first described. Next, optical absorption and cyclic voltammetry measurements are detailed for PProDOT-OC6, PProDOT-OC10, and PProDOT-OEG_3 comparing the effects of the polymerization conditions on the optical and electrochemical properties.

Polymer synthesis

The polymer synthesis of PProDOT-OC6, PProDOT-OC10, and PProDOT-OG_3 *via* mechanochemical oxidative polymerization is detailed in Scheme 1 with the polymerization outcomes provided in Table 1 (complete experimental details of the monomer and polymer synthesis and purification are provided in the ESI†). To first optimize the mechanochemical oxidative polymerization conditions, PProDOT-OC6 was initially targeted (entries 1–7 of Table 1).

A typical polymerization proceeded under ambient conditions where a 10 mL ZrO_2 lined milling jar was charged with the monomer, oxidant, NaCl additive, and a 10 mm ZrO_2 milling ball. The top of the jar was then attached, and the polymerization proceeded in a mixer mill at 30 Hz for a set time (30–120 min). ZrO_2 was selected as the appropriate material for this study, since it is highly corrosion resistant and is harder than other milling jar materials, *e.g.* stainless-steel, allowing for efficient transfer of impact energy between the milling ball, monomer, and chemical oxidant.[44] The corrosion resistance of ZrO_2 is also of particular significance,

Table 1 Mechanochemical oxidative polymerization conditions for the synthesis of PProDOT-OC6, PProDOT-OC10, and PProDOT-OEG_3

Entry	Polymer	Oxidant (equiv.)	Time (h)	M_n[a] (kg mol^{-1}); $Đ$[a]	Yield[a] (%)	λ_{max} (nm); E_g[b] (eV)	HOMO[c]/LUMO[d] (eV)
1	PProDOT-OC6	$FeCl_3$ (6)	1	16.9; 1.18	46	544; 1.97	−4.80/−2.85
2	PProDOT-OC6	$FeCl_3$ (3)	1	15.3; 1.23	10	548; 1.95	−4.74/−2.79
3	PProDOT-OC6	$FeCl_3$ (6)	0.5	12.0; 1.23	7	544; 1.96	−4.80/−2.84
4	PProDOT-OC6	$Fe(OTs)_3$ (6)	1	9.0, 1.18	33	502; 1.92	−4.83/−2.91
5[e]	PProDOT-OC6	$FeCl_3$ (5)	4	12.2; 1.25	43	549; 1.98	−4.82/−2.84
6[f]	PProDOT-OC6	$FeCl_3$ (6)	1	1.1; 3.18	30	544; 1.97	−4.77/−2.80
7	PProDOT-OC6	$FeCl_3$ (6)	2	1.3; 3.08	32	514; 1.97	−4.80/−2.83
8	PProDOT-OC10	$FeCl_3$ (6)	1	14.0; 1.33	44	550; 1.97	−4.97/−2.85
9	PProDOT-OEG_3	$FeCl_3$ (6)	1	7.6; 1.11	32	600; 1.95	−4.97/−3.03

[a] Measured following purification of the polymer product *via* washing with MeOH and hexanes. [b] Calculated using the equation $E_g = 1240/\lambda_{onset}$. [c] Estimated using the equation $E_{HOMO} = -E_{ox}^{onset} - 4.8$ eV. [d] Estimated using the equation $E_{LUMO} = E_{HOMO} + E_g$. [e] Synthesized using solvent based polymerization conditions adapted from ref. 51. [f] No NaCl included.

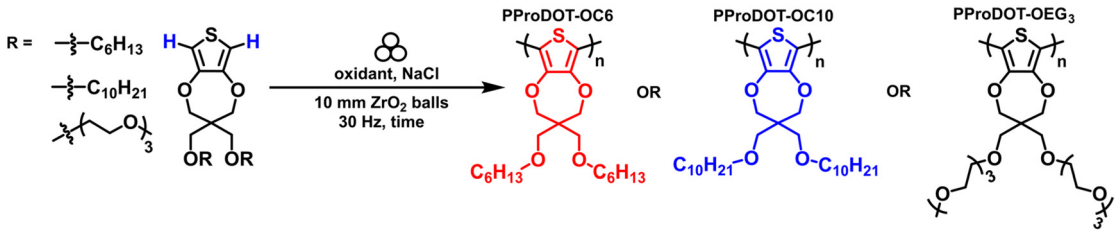

Scheme 1 Synthesis of PProDOT-OC6, PProDOT-OC10, and PProDOT-OEG_3 *via* mechanochemical oxidative polymerization.

Published on 28 January 2025. Downloaded by NIMS SENGEN LIB on 2/12/2025 4:19:03 AM.

since the acidic by-products from the oxidative polymerization, *e.g.* HCl, could corrode and compromise the integrity of a stainless-steel milling jar. The 10 mm diameter milling ball was selected over a smaller sized milling ball, since it allows for increased impact, which has been shown to increase yields and polymer M_n.[41] The frequency of 30 Hz was selected, since previous studies on mechanochemical polymerizations and small-molecule syntheses have shown that a higher frequency, *e.g.* 30 Hz, provides desirable reaction outcomes including higher M_n and yields.[41,59,60] Although, it should be noted that high frequencies (≥20 Hz) for prolonged milling times could lead to polymer chain scission, which is also reported here (*vide infra*).[47,59] NaCl was used as an inert additive allowing for efficient mixing and preventing agglomeration of the polymerization mixture.[45] Note, the polymer yields and M_n/$Đ$ reported in Table 1 were obtained following purification with MeOH and hexanes where MeOH and hexanes remove oligomers, and the hexanes insoluble fraction was collected unless noted otherwise.

Provided with entry 1 of Table 1, 6 equiv. of $FeCl_3$ and a milling time of 1 h afforded PProDOT-OC6 with a desirable M_n of 16.9 kg mol^{-1}, $Đ$ = 1.18, and yield of 46% following purification. Note, an M_n > 10 kg mol^{-1} is desired for polythiophenes, since this is the M_n where their optical and electronic properties begin to saturate.[61] Next, the effect of lowering the amount of oxidant to 3 equiv. of $FeCl_3$ (entry 2 of Table 1) and decreasing the polymerization time from 1 h to 30 min (entry 3 of Table 1) was determined. In both cases, a diminished yield (10% and 7%, respectively) and slight reduction in M_n (15.3 and 12.0 kg mol^{-1}) were obtained with identical $Đ$ of 1.23. The identity of the chemical oxidant was found to be of major significance (entry 4 of Table 1), since employing $Fe(OTs)_3$ in place of $FeCl_3$ led to a reduction in M_n (9.0 kg mol^{-1}) and yield (33%). It was also found that reduction of PProDOT-OC6 synthesized using $Fe(OTs)_3$ with $N_2H_4{\cdot}H_2O$ was less efficient than when $FeCl_3$ was employed as the oxidant due to the presence of insoluble polymer material and broadened, partially quenched ^{1}H-NMR resonances (Fig. S8†), likely indicating the presence of radical cations present within the polymer π-conjugated backbone.[62] The effect of the NaCl additive was also assessed, and it was found that exclusion of NaCl (entry 6 of Table 1) afforded lower M_n (1.1 kg mol^{-1}), decreased yield (30%), and broader $Đ$ (3.18). This significant change in the polymerization outcome reflects the critical role of NaCl to promote efficient mixing of the monomer and oxidant and limit agglomeration.[45,63] To determine if longer milling time leads to depolymerisation, the polymerization time was extended to 2 h (entry 7 of Table 1), and it was found that doubling the milling time leads to a significant decrease in M_n (1.3 kg mol^{-1}), lower yield (30%), and broader $Đ$ (3.08). Optimization of the milling time for mechanochemical polymerizations is critical and must be finely balanced to maximize yields and polymer M_n, while avoiding mechanochemically induced polymer chain scission.[59] Based on the results from optimizing the polymerization conditions, it was confirmed that a polymerization time of 1 h with 6 equiv. of $FeCl_3$ oxidant afforded the optimal polymerization outcome.

Notably, the M_n and yield for the mechanochemically synthesized PProDOT-OC6 reported here indicate a comparable outcome to the solvent based oxidative polymerization (entry 5 of Table 1), which afforded PProDOT-OC6 in 43% yield with a M_n of 12.2 kg mol^{-1} and $Đ$ = 1.25, and with previous literature reports for PProDOT analogues (Fig. 2A).[51]

Regarding differences in polymerization mechanism between the solvent based and mechanochemical oxidative polymerization, there is not a clear indication that the absence of solvent alters the radical based step-growth type mechanism. Specifically, there is no dependence between the equivalents of oxidant used (initiator) and the polymer M_n where a decrease in the amount of $FeCl_3$ employed does not lead to an increase in M_n, which would be consistent with a chain-growth or controlled polymerization mechanism. While the $Đ$ is narrow for PProDOT-OC6 synthesized here, narrow $Đ$ ($Đ$ < 2) has been reported for PProDOT analogues synthesized *via* oxidative polymerization and DArP (Fig. 2A).[51,57]

To confirm the structural fidelity of mechanochemically synthesized PProDOT-OC6 is maintained, the ^{1}H-NMR spectrum was recorded and compared to the spectrum of PProDOT-OC6 synthesized using solvent-based oxidative polymerization (Fig. 3). For both the mechanochemical and solvent based polymer batches, there is an absence of any end-groups or aromatic ^{1}H resonances corresponding to the monomer *circa* 6.44 ppm (Fig. S1 in ESI†). The resonances for PProDOT-OC6 synthesized mechanochemically indicate increased broadening likely due to the higher M_n achieved for the polymer (16.9 kg mol^{-1} *versus* 12.2 kg mol^{-1}; see Fig. S12 in ESI†), and the ^{1}H resonances corresponding to the 3,4-propylenedioxy ring (H_a–$H_{b'}$ *circa* 4.15–3.43 ppm) and the *n*-hexyl sidechain (H_c–$H_{h'}$ *circa* 1.56–0.89 ppm) show similar line shapes and multiplicity as broad singlets. Notably, the appear-

This journal is © The Royal Society of Chemistry 2025

Published on 28 January 2025. Downloaded by NIMS SENGEN LIB on 2/12/2025 4:19:03 AM.

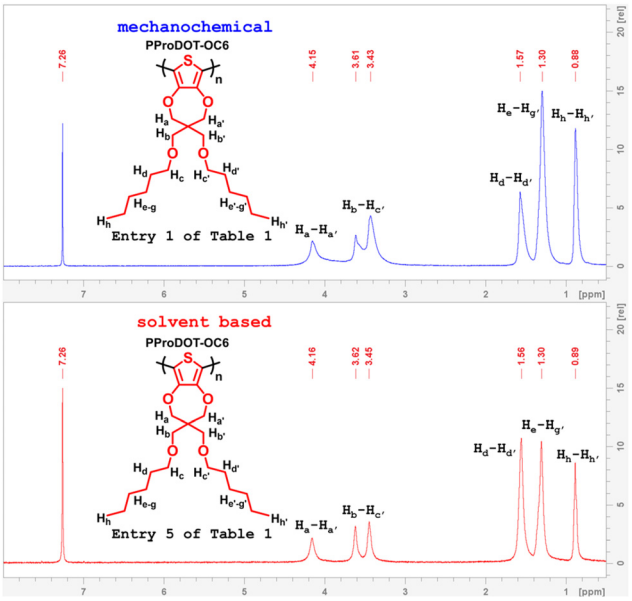

Fig. 3 ^{1}H-NMR spectra of PProDOT-OC6 synthesized *via* mechanochemical oxidative polymerization (top) and solvent based oxidative polymerization (bottom). Collected in $CDCl_3$ at 25 °C.

ance of resonances corresponding to aldehydes and ketone based defects (~2.1, 3.0, 3.47, and 8.3 ppm), which have been reported for PProDOT analogues synthesized *via* DArP, are absent.[64]

Next, the effect of the monomer sidechain identity on the polymerization outcome was determined using the optimal polymerization conditions provided with entry 1 of Table 1 (6 equiv. of $FeCl_3$ and a polymerization time of 1 h). Polymerization of ProDOT-OC10 employing an extended n-decyloxy sidechain provided a comparable yield (44%), M_n (14.0 kg mol^{-1}), and narrow $Đ$ (1.33) relative to PProDOT-OC6 (entry 8 of Table 1). Lastly, incorporation of EG_3 sidechains with ProDOT-OEG_3 lead to slight reduction in yield (32%) and M_n (7.6 kg mol^{-1}), but a narrow $Đ$ (1.11) was maintained (entry 9 of Table 1).

Cyclic voltammetry and optical absorption

Polymer cyclic voltammetry (CV) measurements were performed using a 3-electrode system under a nitrogen atmosphere with a polymer coated glassy carbon working electrode, a Ag-wire pseudo-reference electrode, and a Ag-wire counter electrode. All measurements were referenced to the ferrocene/ferrocenium (Fc/Fc^+) redox couple. Polymer films were subjected to electrochemical conditioning prior to recording the voltammogram to ensure changes in the polymer morphology/microstructure *via* electrolyte penetration and exchange did not influence measurement outcomes and analysis.[65] Cyclic voltammograms are provided in Fig. 4A and Fig. S14† with the estimated HOMO/LUMO energy levels tabulated in Table 1. From inspection of the PProDOT-OC6 CV traces, there is a clear dependence of the polymerization conditions employed on the electrochemical oxidation of the polymers. Specifically,

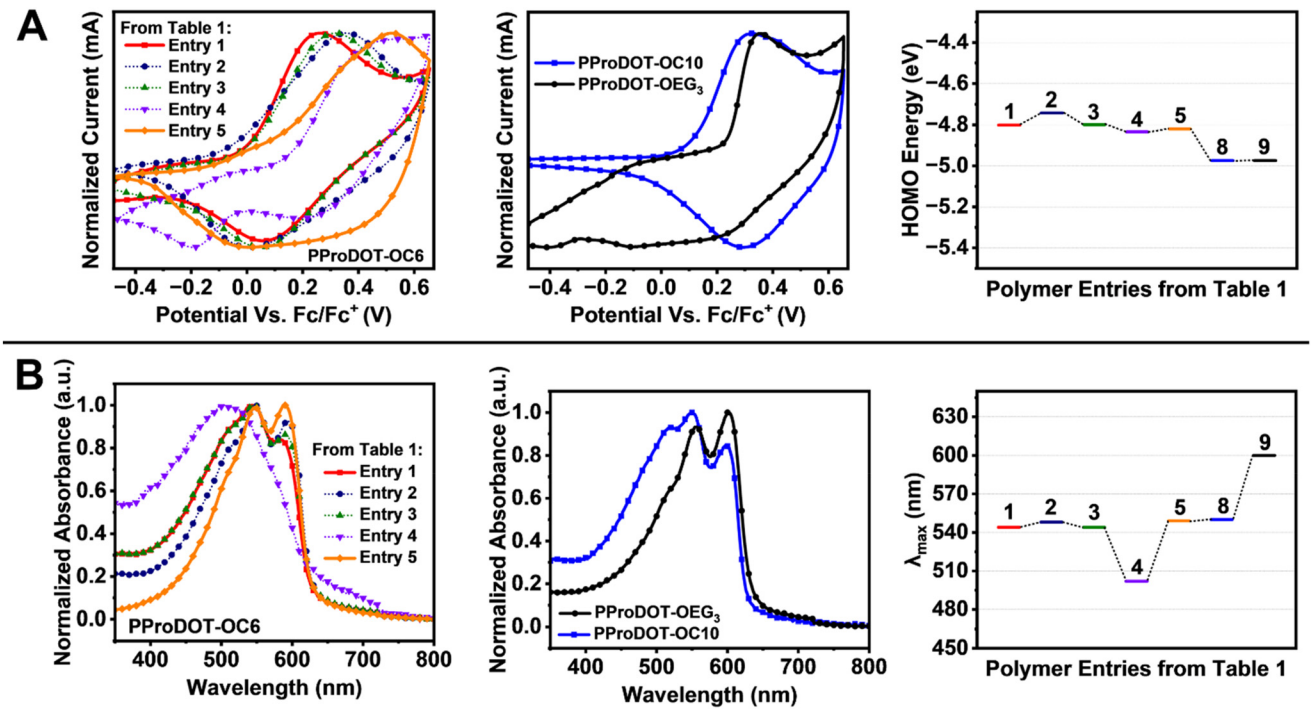

Fig. 4 (A) Cyclic voltammograms for PProDOT-OC6 (entries 1–5 of Table 1), PProDOT-OC10 (entry 8 of Table 1), PProDOT-OEG_3 (entry 9 of Table 1), and the relative HOMO energy levels for each polymer. (B) Thin-film optical absorption spectra for PProDOT-OC6 (entries 1–5 of Table 1), PProDOT-OC10 (entry 8 of Table 1), PProDOT-OEG_3 (entry 9 of Table 1), and the relative optical bandgaps (E_g) for each polymer.

Published on 28 January 2025. Downloaded by NIMS SENGEN LIB on 2/12/2025 4:19:03 AM.

reversible oxidations are observed for PProDOT-OC6 corresponding to entries 1–3 of Table 1, but for the PProDOT-OC6 batch corresponding to entry 4 of Table 1 where $Fe(OTs)_3$ is employed as the oxidant an irreversible oxidation is observed. This deviation in the electrochemical properties of the polymer is attributed to the lower polymer M_n and potential trapping of $Fe(OTs)_3$ residues. This is indicated further with the optical absorption spectrum (Fig. 4B) and observed quenching of the ^{1}H-NMR resonances (Fig. S8†). The CV trace for PProDOT-OC6 synthesized *via* solvent-based oxidative polymerization (entry 5 of Table 1) shows the desired reversible oxidation (Fig. 4A), and all estimated HOMO energy levels for the different PProDOT-OC6 batches are within a proximal range (−4.74 to −4.83 eV). For PProDOT-C10 and PProDOT-OEG_3, estimated HOMO energy levels were found to be identical at −4.97 eV.

PProDOT-OC6 polymers synthesized using $FeCl_3$ as the oxidant (entries 1–3 and 5–7 of Table 1) show comparable optical absorption extending from ∼450–625 nm with similar λ_{max} = 544–549 nm providing optical bandgaps (E_g) within a narrow range from 1.95–1.98 eV (Fig. 4B and Fig. S14†). A vibronic shoulder *circa* 590 nm is also apparent for each of these entries indicating improved self-assembly of the regiosymmetric PProDOT-OC6 polymer chains demonstrating excellent structural fidelity.[56,66,67] PProDOT-OC6 synthesized using $Fe(OTs)_3$ (entry 4 of Table 1) shows a broad featureless absorption band extending from ∼400–600 nm with λ_{max}/E_g of 502 nm/1.92 eV. This significant blue shift (42 nm) is likely due to the lower M_n of the polymer (9.0 kg mol^{-1} *versus* 16.9 kg mol^{-1} for entry 1 of Table 1). For PProDOT-OC10/PProDOT-OEG_3, similar optical absorption profiles are observed (λ_{max} = 550/600 nm, respectively) as well as optical bandgaps (E_g = 1.95/1.97 eV, respectively). The significant redshift for PProDOT-OEG_3 (50 nm) has been observed with other PProDOT analogues incorporating EG_n based sidechains, and this can be attributed to a strong vibronic shoulder indicative of improved polymer self-assembly and increased sidechain interdigitation characteristic of linear EG_n based sidechains.[65,68]

Experimental

Materials and methods

All reactions were performed under dry N_2 in oven dried glassware, unless otherwise noted. All reagents and solvents were purchased and used as received from commercial sources: Fisher Scientific, VWR, Ambeed, and Sigma Aldrich. Mechanochemical polymerizations were performed using a Retsch MM-400 mixer mill using 10 mL zirconia lined jars (cat.# 014620234) and 10 mm diameter zirconia grinding balls (cat.# 053680094) under ambient conditions. Ethyl acetate (EtOAc) used for the solvent based oxidative polymerization was dried by storing over activated 3 Å molecular sieves overnight.

General procedure for mechanochemical oxidative polymerization

Under ambient conditions, a 10 mL stainless steel jar lined with zirconia was charged with 0.52 mmol (1 equiv.) of monomer (S4–S6), $FeCl_3$ (506.1 mg, 3.12 mmol, 6 equiv.), NaCl (1.00 g, 17.1 mmol, 32.9 equiv.), and a 10 mm diameter zirconia ball. The jar was then sealed with a screw-cap and subjected to 1 h. of mixing at 30 Hz. Then to purify the crude polymer product it was first dissolved in toluene (20 mL) and washed with DI–H_2O (30 mL). The toluene layer was collected, and $N_2H_4{\cdot}H_2O$ (5 mL) was then added to reduce the oxidized polymer. This mixture was allowed to stir at room temperature for 1 h. A noticeable colour change occurred during this time from green to bright red. The mixture was then washed with DI–H_2O (20 mL), the toluene layer was collected, and the solvent evaporated under reduced pressure. The solid was then dissolved in a minimal amount of toluene (2 mL) and this was slowly precipitated into chilled methanol with rapid stirring. After stirring for 20 min the precipitate was collected *via* filtration onto a nylon membrane. The precipitate was washed with methanol (5 × 10 mL) and hexane (5 × 10 mL). The polymer was dried overnight under vacuum prior to analysis.

General procedure for solvent based oxidative polymerization

Adapted from literature.[51] Monomer S4 (200 mg, 0.52 mmol, 1 equiv.) and anhydrous EtOAc (2.5 mL) were added to a one-neck round bottom flask equipped with a stir bar. The solution was stirred and degassed *via* bubbling with nitrogen for 45 minutes. In a separate round bottom flask, $FeCl_3$ (421.72 mg, 2.6 mmol, 5 equiv.) was dissolved in anhydrous EtOAc (1 mL), and this solution was purged with nitrogen for 5 min. The monomer solution was then added dropwise in $FeCl_3$ solution. The mixture was stirred vigorously while being continuously bubbled with nitrogen for 3 h. after which the green suspension was poured into methanol (100 mL). The green precipitate was stirred for 45 minutes, filtered onto a nylon membrane, and washed with methanol (50 mL). The precipitate was then dissolved using toluene (4 mL), treated with $N_2H_4{\cdot}H_2O$ (5 mL), and then stirred for one hour. The pink toluene solution was poured into a separatory funnel and washed with water (50 mL) three times. The toluene fraction was then collected, and the volume was reduced to 2 mL under reduced pressure. The concentrated toluene fraction was then precipitated into methanol (150 mL) and stirred for 45 minutes. The purple precipitate was then filtered onto a nylon membrane, and polymer was washed with methanol (5 × 10 mL) and hexane (5 × 10 mL) to afford the polymer as a purple solid. The polymer was dried overnight under vacuum prior to analysis.

Cyclic voltammetry

Cyclic voltammetry was performed using a BioLogic SP-50e potentiostat controlled using EC-Labs software. Electrochemical measurements proceeded using an oven-dried, 10 ml 3-neck round-bottom flask under nitrogen atmosphere. Electrolyte solutions (0.1 M Bu_4NPF_6 in MeCN) were

 This journal is © The Royal Society of Chemistry 2025

Published on 28 January 2025. Downloaded by NIMS SENGEN LIB on 2/12/2025 4:19:03 AM.

prepared in a nitrogen glovebox. The cell was set up in a three-electrode system using a Ag-wire as a pseudo-reference electrode (RE), platinum wire for the counter electrode (CE) and a glassy carbon as the working electrode (WE). 10 mg mL^{-1} polymer–CF solutions were drop-casted onto a polished WE to yield the polymer films. The electrochemical cell was degassed with nitrogen for 10 minutes prior to measurement. Polymer films were electrochemically conditioned by cycling from 0 to +1.5 V at 100 mV s^{-1} 10×. All measurements were referenced to Fc/Fc^{+}. HOMO and LUMO energy levels were estimated using the equations $E_{HOMO} = -E_{ox}^{onset} - 4.80$ eV and $E_{LUMO} = E_{HOMO} + E_g^{opt}$.

Optical absorption spectroscopy

Optical absorption measurements were performed using a Shimadzu UV-3600 I Plus spectrophotometer. Polymer thin-film measurements were performed using glass slide substrates, which were cleaned *via* sonication in DI–H_2O, followed by aqueous detergent, MeOH, 2-propanol, and acetone. The slides were then dried overnight (16 h.) in an oven (120 °C). The films were spin-coated onto the cleaned glass slides using 10 mg ml^{-1} polymer/CF solutions at 3000 rpm and thermally annealed in a glovebox on a hotplate at 100 °C for 10 min. E_g^{opt} was estimated using the equation $E_g^{opt} = 1240/\lambda_{onset}$.

Conclusions

In this work, the development of robust mechanochemical oxidative polymerization conditions towards the synthesis of PProDOT analogues is described. The polymerization proceeds in the absence of solvent and without the application of external heating employing only the monomer, oxidant, milling jar and ball, and NaCl as an inert additive affording polymers with M_n up to 16.9 kg mol^{-1} and yields up to 46%, which are comparable to yields obtained using solvent based polymerizations (12.2 kg mol^{-1} and 43%). The mechanochemical polymerization conditions were first optimized using ProDOT-OC6 as the monomer to yield PProDOT-OC6, which contains an *n*-hexyloxy sidechain. The equivalents of oxidant (6 equiv. or 3 equiv.), milling time (1 or 0.5 h), and identity of the oxidant ($FeCl_3$ or $Fe(OTs)_3$) were optimized with 6 equiv. of $FeCl_3$ and a milling time of 1 h providing the optimal polymerization outcome. The PProDOT polymers were characterized using ^{1}H-NMR, optical absorption spectroscopy, and cyclic voltammetry to ensure desirable structural fidelity and optical and electrochemical properties were obtained. It was found that the identity of the oxidant [$FeCl_3$ *versus* $Fe(OTs)_3$] played a critical role in the polymerization outcome (M_n of 16.9 kg mol^{-1} *versus* 9.0 kg mol^{-1} and yields of 46% and 33%, respectively) and determining the optical properties of the polymer (λ_{max} of 544 nm *versus* 502 nm). To demonstrate the broader scope of these polymerization conditions towards PProDOT analogues with extended (*n*-decyloxy) or EG_n based sidechains (EG_3) PProDOT-OC10 and PProDOT-OEG_3 were synthesized in acceptable M_n (14.0 and 7.6 kg mol^{-1}) and yields (44 and 32%). Overall, these findings demonstrate a sustainable approach towards the synthesis of PProDOT analogues compared to typical polymerization methodologies which require toxic, hazardous solvents and high temperatures ($T \geq 100$ °C).

Author contributions

Conceptualization: T. Z., R. R., and R. P.; investigation, methodology and data acquisition and curation: T. Z., R. R., and A. M.; writing—original draft: T. Z. and R. R.; writing—review and editing: T. Z., R. R., A. M., and R. P.; funding acquisition: R. P. The manuscript was written through contributions of all authors. All authors have approved the final version of the manuscript.

Data availability

The data supporting the findings of this article have been included within the article and the ESI.†

Conflicts of interest

There are no conflicts to declare.

Acknowledgements

The authors gratefully acknowledge support from the UT System STARS Program, UTEP University Research Institute, and UTEP Startup Awards.

References

1 G. Zhang, F. R. Lin, F. Qi, T. Heumüller, A. Distler, H.-J. Egelhaaf, N. Li, P. C. Y. Chow, C. J. Brabec, A. K.-Y. Jen and H.-L. Yip, *Chem. Rev.*, 2022, **122**, 14180–14274.
2 C. An, Z. Zheng and J. Hou, *Chem. Commun.*, 2020, **56**, 4750–4760.
3 K. A. Mazzio and C. K. Luscombe, *Chem. Soc. Rev.*, 2015, **44**, 78–90.
4 A. Giovannitti, R. B. Rashid, Q. Thiburce, B. D. Paulsen, C. Cendra, K. Thorley, D. Moia, J. T. Mefford, D. Hanifi, D. Weiyuan, M. Moser, A. Salleo, J. Nelson, I. McCulloch and J. Rivnay, *Adv. Mater.*, 2020, **32**, 1908047.
5 J. Kim, R. M. Pankow, Y. Cho, I. D. Duplessis, F. Qin, D. Meli, R. Daso, D. Zheng, W. Huang, J. Rivnay, T. J. Marks and A. Facchetti, *Nat. Electron.*, 2024, **7**, 234–243.
6 A. Erhardt, A. Hochgesang, C. R. McNeill and M. Thelakkat, *Adv. Electron. Mater.*, 2023, **9**, 2300026.
7 P. Das, R. Elizalde-Segovia, B. Zayat, C. Z. Salamat, G. Pace, K. Zhai, R. C. Vincent, B. S. Dunn, R. A. Segalman,

Published on 28 January 2025. Downloaded by NIMS SENGEN LIB on 2/12/2025 4:19:03 AM.

S. H. Tolbert, S. R. Narayan and B. C. Thompson, *Chem. Mater.*, 2022, **34**, 2672–2686.
8 P. Das, C. Z. Salamat, B. Zayat, R. Elizalde-Segovia, Y. Wang, X. Gu, S. R. Narayan, S. H. Tolbert and B. C. Thompson, *Chem. Mater.*, 2024, **36**, 1413–1427.
9 D. T. McQuade, A. E. Pullen and T. M. Swager, *Chem. Rev.*, 2000, **100**, 2537–2574.
10 T. Zubair, M. M. Hasan, R. S. Ramos and R. M. Pankow, *J. Mater. Chem. C*, 2024, **12**, 8188–8216.
11 P. M. Beaujuge and J. R. Reynolds, *Chem. Rev.*, 2010, **110**, 268–320.
12 X. Li, K. Perera, J. He, A. Gumyusenge and J. Mei, *J. Mater. Chem. C*, 2019, **7**, 12761–12789.
13 T. Bura, J. T. Blaskovits and M. Leclerc, *J. Am. Chem. Soc.*, 2016, **138**, 10056–10071.
14 L. Ye and B. C. Thompson, *J. Polym. Sci.*, 2022, **60**, 393–428.
15 R. M. Pankow and B. C. Thompson, *Polymer*, 2020, **207**, 122874.
16 M. P. Aplan and E. D. Gomez, *Ind. Eng. Chem. Res.*, 2017, **56**, 7888–7901.
17 K. Okamoto, J. Zhang, J. B. Housekeeper, S. R. Marder and C. K. Luscombe, *Macromolecules*, 2013, **46**, 8059–8078.
18 L. Ye and B. C. Thompson, *ACS Macro Lett.*, 2021, **10**, 714–719.
19 C. Capello, U. Fischer and K. Hungerbuhler, *Green Chem.*, 2007, **9**, 927–934.
20 C. K. Lo, R. M. W. Wolfe and J. R. Reynolds, *Chem. Mater.*, 2021, **33**, 4842–4852.
21 A. Uva, A. Lin and H. Tran, *J. Am. Chem. Soc.*, 2023, **145**, 3606–3614.
22 L.-P. Boivin, W. Dupont, D. Gendron and M. Leclerc, *Macromol. Chem. Phys.*, 2023, **224**, 2200378.
23 L. Xing and C. K. Luscombe, *J. Mater. Chem. C*, 2021, **9**, 16391–16409.
24 G. E. Castillo and B. C. Thompson, *ACS Macro Lett.*, 2023, **12**, 1339–1344.
25 G. Forti, R. M. Pankow, F. Qin, Y. Cho, B. Kerwin, I. Duplessis, A. Nitti, S. Jeong, C. Yang, A. Facchetti, D. Pasini and T. J. Marks, *Chem. – Eur. J.*, 2023, **29**, e202300653.
26 N. Nozaki, A. Uva, H. Matsumoto, H. Tran and M. Ashizawa, *RSC Appl. Polym.*, 2024, **2**, 163–171.
27 K. A. Bartlett, A. Charland-Martin, J. Lawton, A. L. Tomlinson and G. S. Collier, *Macromol. Rapid Commun.*, 2024, **45**, 2300220.
28 Y. Mohr, A. Ranscht, M. Alves-Favaro, E. Alessandra Quadrelli, F. M. Wisser and J. Canivet, *Chem. – Eur. J.*, 2023, **29**, e202202667.
29 N. R. Kakde and S. K. Asha, *Polym. Chem.*, 2023, **14**, 2803–2819.
30 R. Matsidik, A. Luzio, S. Hameury, H. Komber, C. R. McNeill, M. Caironi and M. Sommer, *J. Mater. Chem. C*, 2016, **4**, 10371–10380.
31 T. J. Aldrich, W. Zhu, S. Mukherjee, L. J. Richter, E. Gann, D. M. DeLongchamp, A. Facchetti, F. S. Melkonyan and T. J. Marks, *Chem. Mater.*, 2019, **31**, 4313–4321.
32 R. M. Pankow, L. Ye, N. S. Gobalasingham, N. Salami, S. Samal and B. C. Thompson, *Polym. Chem.*, 2018, **9**, 3885–3892.
33 A. Sanzone, A. Calascibetta, M. Monti, S. Mattiello, M. Sassi, F. Corsini, G. Griffini, M. Sommer and L. Beverina, *ACS Macro Lett.*, 2020, **9**, 1167–1171.
34 C. Zhu, L. Liu, Q. Yang, F. Lv and S. Wang, *Chem. Rev.*, 2012, **112**, 4687–4735.
35 Q. Li, J.-D. Huang, T. Liu, T. P. A. van der Pol, Q. Zhang, S. Y. Jeong, M.-A. Stoeckel, H.-Y. Wu, S. Zhang, X. Liu, H. Y. Woo, M. Fahlman, C.-Y. Yang and S. Fabiano, *J. Am. Chem. Soc.*, 2024, **146**, 15860–15868.
36 P. T. Anastas and J. C. Warner, *Green Chemistry: Theory and Practice*, Oxford University Press, 2000.
37 N. Fantozzi, J.-N. Volle, A. Porcheddu, D. Virieux, F. García and E. Colacino, *Chem. Soc. Rev.*, 2023, **52**, 6680–6714.
38 T. Friščić, C. Mottillo and H. M. Titi, *Angew. Chem., Int. Ed.*, 2020, **59**, 1018–1029.
39 S. L. James, C. J. Adams, C. Bolm, D. Braga, P. Collier, T. Friščić, F. Grepioni, K. D. M. Harris, G. Hyett, W. Jones, A. Krebs, J. Mack, L. Maini, A. G. Orpen, I. P. Parkin, W. C. Shearouse, J. W. Steed and D. C. Waddell, *Chem. Soc. Rev.*, 2012, **41**, 413–447.
40 L. P. T. Nirmani, F. F. Pary and T. L. Nelson, *Green Chem. Lett. Rev.*, 2022, **15**, 863–868.
41 J. B. Ravnsbæk and T. M. Swager, *ACS Macro Lett.*, 2014, **3**, 305–309.
42 A. Krusenbaum, S. Grätz, G. T. Tigineh, L. Borchardt and J. G. Kim, *Chem. Soc. Rev.*, 2022, **51**, 2873–2905.
43 S. Grätz and L. Borchardt, *RSC Adv.*, 2016, **6**, 64799–64802.
44 S. Grätz, B. Wolfrum and L. Borchardt, *Green Chem.*, 2017, **19**, 2973–2979.
45 S. Grätz, M. Oltermann, E. Troschke, S. Paasch, S. Krause, E. Brunner and L. Borchardt, *J. Mater. Chem. A*, 2018, **6**, 21901–21905.
46 P. Chakma, S. M. Zeitler, F. Baum, J. Yu, W. Shindy, L. D. Pozzo and M. R. Golder, *Angew. Chem., Int. Ed.*, 2023, **62**, e202215733.
47 C. Oh, E. H. Choi, E. J. Choi, T. Premkumar and C. Song, *ACS Sustainable Chem. Eng.*, 2020, **8**, 4400–4406.
48 R. C. So and A. C. Carreon-Asok, *Chem. Rev.*, 2019, **119**, 11442–11509.
49 I. Osaka and R. D. McCullough, *Acc. Chem. Res.*, 2008, **41**, 1202–1214.
50 C. M. Amb, J. A. Kerszulis, E. J. Thompson, A. L. Dyer and J. R. Reynolds, *Polym. Chem.*, 2011, **2**, 812–814.
51 J. Padilla, A. M. Österholm, A. L. Dyer and J. R. Reynolds, *Sol. Energy Mater. Sol. Cells*, 2015, **140**, 54–60.
52 Y. Zhang, L. Kong, Y. Zhang, H. Du, J. Zhao, S. Chen, Y. Xie and Y. Wang, *Org. Electron.*, 2020, **81**, 105685.
53 L. M. Campos, A. J. Mozer, S. Günes, C. Winder, H. Neugebauer, N. S. Sariciftci, B. C. Thompson, B. D. Reeves, C. R. G. Grenier and J. R. Reynolds, *Sol. Energy Mater. Sol. Cells*, 2006, **90**, 3531–3546.
54 J. F. Ponder Jr., A. K. Menon, R. R. Dasari, S. L. Pittelli, K. J. Thorley, S. K. Yee, S. R. Marder and J. R. Reynolds, *Adv. Energy Mater.*, 2019, **9**, 1900395.

 This journal is © The Royal Society of Chemistry 2025

Published on 28 January 2025. Downloaded by NIMS SENGEN LIB on 2/12/2025 4:19:03 AM.

55 L. R. Savagian, A. M. Österholm, J. F. Ponder Jr., K. J. Barth, J. Rivnay and J. R. Reynolds, *Adv. Mater.*, 2018, **30**, 1804647.
56 B. D. Reeves, C. R. G. Grenier, A. A. Argun, A. Cirpan, T. D. McCarley and J. R. Reynolds, *Macromolecules*, 2004, **37**, 7559–7569.
57 H. Zhao, C.-Y. Liu, S.-C. Luo, B. Zhu, T.-H. Wang, H.-F. Hsu and H. Yu, *Macromolecules*, 2012, **45**, 7783–7790.
58 A. Kumar, R. Singh, S. P. Gopinathan and A. Kumar, *Chem. Commun.*, 2012, **48**, 4905–4907.
59 H. Y. Cho and C. W. Bielawski, *Angew. Chem., Int. Ed.*, 2020, **59**, 13929–13935.
60 T. Seo, K. Kubota and H. Ito, *J. Am. Chem. Soc.*, 2023, **145**, 6823–6837.
61 P. Schilinsky, U. Asawapirom, U. Scherf, M. Biele and C. J. Brabec, *Chem. Mater.*, 2005, **17**, 2175–2180.
62 Y. Kim, Y.-J. Kim, Y.-A. Kim, E. Jung, Y. Mok, K. Kim, H. Hwang, J.-J. Park, M.-G. Kim, S. Mathur and D.-Y. Kim, *ACS Appl. Mater. Interfaces*, 2021, **13**, 2887–2898.
63 L. Konnert, A. Gauliard, F. Lamaty, J. Martinez and E. Colacino, *ACS Sustainable Chem. Eng.*, 2013, **1**, 1186–1191.
64 G. S. Collier and J. R. Reynolds, *ACS Macro Lett.*, 2019, **8**, 931–936.
65 A. A. Advincula, A. L. Jones, K. J. Thorley, A. M. Österholm, J. F. Ponder and J. R. Reynolds, *Chem. Mater.*, 2022, **34**, 4633–4645.
66 N. S. Gobalasingham, J. E. Carle, F. C. Krebs, B. C. Thompson, E. Bundgaard and M. Helgesen, *Macromol. Rapid Commun.*, 2017, **38**, 1700526.
67 F. Livi, N. S. Gobalasingham, B. C. Thompson and E. Bundgaard, *J. Polym. Sci., Part A:Polym. Chem.*, 2016, **54**, 2907–2918.
68 R. M. Pankow, B. Kerwin, Y. Cho, S. Jeong, G. Forti, B. Musolino, C. Yang, A. Facchetti and T. J. Marks, *Adv. Funct. Mater.*, 2023, **34**, 2309428.